Original article

Folia Neuropathologica

Size frequency distributions of abnormal protein deposits in Alzheimer's disease and variant Creutzfeldt-Jakob disease

Richard A. Armstrong

Vision Sciences, Aston University, Birmingham, UK

Folia Neuropathol 2007; 45 (3): 108-114

Abstract

The size frequency distributions of β-amyloid (Aβ) and prion protein (PrP^{sc}) deposits were studied in Alzheimer's disease (AD) and the variant form of Creutzfeldt-Jakob disease (vCJD) respectively. All size distributions were unimodal and positively skewed. Aβ deposits reached a greater maximum size and their distributions were significantly less skewed than the PrP^{sc} deposits. All distributions were approximately log-normal in shape but only the diffuse PrP^{sc} deposits did not deviate significantly from a log-normal model. There were fewer larger classic Aβ deposits than predicted and the florid PrP^{sc} deposits occupied a more restricted size range than predicted by a log-normal model. Hence, Aβ deposits exhibit greater growth than the corresponding PrP^{sc} deposits. Surface diffusion may be particularly important in determining the growth of the diffuse PrP^{sc} deposits. In addition, there are factors limiting the maximum size of the Aβ and florid PrP^{sc} deposits.

Key words: *β-amyloid (Aβ), prion protein (PrP^{sc}), size distribution, log-normal distribution, surface diffusion, protein deposit growth.*

Introduction

There are similarities in the pathology of Alzheimer's disease (AD) and Creutzfeldt-Jakob disease (CJD) [7,20]. Both disorders are characterized by the deposition of a protease resistant protein aggregate in the form of deposits or plaques, viz., β-amyloid (Aβ) in AD and the disease associated form of prion protein (PrP^{sc}) in CJD. In some patients, Aβ and prion pathology can even coexist [20,32,34], with in one reported family the features of both CJD and AD pathology linked to a presenilin 1 (PSEN1) mutation [19]. In addition, Aβ and PrP^{sc} deposits exhibit similarities in spatial topography, being distributed in clusters that in the cerebral cortex are regularly distributed parallel to the pia mater [7].

Aβ is generated via β and γ-secretase cleaving of amyloid precursor protein (APP), while PrP^{sc} is an abnormal structural conformation of normal cellular PrP (PrP^{c}) and results from the autocatalytic conversion of PrP^{c} to PrP^{sc}. The formation of protein aggregates is a nucleated polymerization reaction with an initial nucleation event (lag phase) followed by the extension of newly formed nuclei into larger aggregates (growth phase) [16,21,29]. Several studies have suggested that Aβ deposits grow in the brain. Pseudocolour image processing reveals gradients of density within Aβ deposits consistent with growth from

Communicating author:

Dr. R.A. Armstrong, Vision Sciences, Aston University, Birmingham, B4 7ET, UK, tel.: 0121 359 36 11, fax: 0121 333 42 20, Email: R.A.Armstrong@aston.ac.uk

a central point [13]. Radioiodinated human Aβ can be deposited experimentally *in vitro* from a dilute solution onto primitive and diffuse deposits, causing them to grow [30]. In transgenic mice, Aβ deposits appear in clusters which grow in size from 14 µm at 8 months to 22 µm at 12 months [41]. Transgenic studies also suggest that increasing accumulation of Aβ is largely by growth of existing deposits rather than by further nucleation [36].

The size frequency distributions of protein deposits in thin sections of tissue have been used to investigate the growth phase [3,23,38]. Hence, in AD and Down's syndrome (DS), Aβ deposits exhibit a unimodal, positively skewed distribution [6,23]. There were few deposits in the smallest size class (plaque diameter <10 µm), maximum frequency occurred between 20 µm and 40 µm (the modal class), and the frequency of the larger deposits declined with increasing size. A log-normal model has been fitted to the size frequency distributions of Aβ deposits in DS [23,38]. This model suggests that after nucleation, the growth phase of the Aβ deposits can be described by a function in which increase in volume of a deposit in a time interval is proportional to its volume at the beginning of the time interval ($dV/dt = K(t)V$, where V = deposit volume and K(t) is a parameter changing randomly around a constant positive value) [23]. Previous studies also suggest that PrP^{sc} deposits in CJD exhibit a size distribution similar to that of Aβ deposits in AD [12]. Hence, the present study compared the size frequency distributions in the temporal lobe of Aβ deposits in AD with deposits of PrP^{sc} in the variant subtype of CJD (vCJD) [8]. Variant CJD is a relatively new form of the disease first described in the UK in 1996 [43] and has protein deposits that morphologically resemble those of AD [8].

Materials and methods

Cases

Ten cases of sporadic AD (Table I) were obtained from the Brain Bank, Department of Neuropathology, Institute of Psychiatry, King's College London, UK, and 11 vCJD cases from the National CJD Surveillance Unit, Western General Hospital, Edinburgh, UK. Informed consent was given for the removal of all brain tissue according to the 1996 Declaration of Helsinki (as modified Edinburgh 2000). The AD cases were clinically assessed and all fulfilled the National Institute of Neurological and Communicative Disorders and Stroke and Alzheimer's Disease and Related Disorders Association (NINCDS/ADRDA) criteria for probable AD [39]. The histological diagnosis of AD was established by the presence of widespread neocortical senile plaques (SP) consistent with the Consortium to Establish a Registry of Alzheimer's Disease (CERAD) criteria [31]. AD cases conformed to stages IV to VI of the Braak system [14]. All CJD cases fulfilled the neuropathological diagnostic criteria for vCJD [24]. None of the cases had any of the known mutations of the *PrP* gene or family history of prion disease, and there was no evidence of the known types of iatrogenic aetiology. The PrP^{sc} characteristic of vCJD has a uniform glycotype (PrP^{sc}, Type 4) and is distinct from that observed in sporadic CJD [22,24].

Histological methods

A block of the temporal cortex was taken from each case at the level of the lateral geniculate nucleus to study the superior temporal gyrus (B22), inferior temporal gyrus (B20), and parahippocampal gyrus (B28). Tissue was fixed in 10% phosphate buffered formal-saline and embedded in paraffin wax. In AD, coronal 7 µm sections were stained with a rabbit polyclonal antibody (provided by Professor B.H. Anderton, Institute of Psychiatry, King's College London) raised against the 12-28 amino acid sequence of the Aβ protein (dilution 1:1200) [37]. In vCJD, coronal 7 µm sections were immunostained against PrP^{sc} using the monoclonal antibody 12F10 (dilution 1:250) that binds to residues 142-160 of human PrP downstream of the neurotoxic domain adjacent to helix region 2 [27] (provided by Prof. G. Hunsmann, The German Primate Centre, Gottingen, Germany). Immunoreactivity was enhanced by formic acid (98% for 5 minutes) and autoclaving (121°C for 10 minutes) pretreatment. Sections were treated with Dako Bioti-

Table I. Details of the Alzheimer's disease and variant Creutzfeldt-disease cases

Patient group	N	M:F	Mean age (years); (range, SD)	Mean duration (years) (range, SD)
Alzheimer's disease	10	2:8	80.2 (64-93, 8.5)	5.9 (2-16, 3.3)
Variant Creutzfeldt-Jakob disease	11	6:5	29.5 (18-48, 9.13)	1.3 (1-2, 0.47)

N – number of cases studied; M – male; F – female; SD – standard deviation.

nylated Rabbit anti-Mouse (RAM) (dilution 1:100) and Dako ABComplex HRP kit for 45 minutes (Amersham, UK). Diaminobenzidine tetrahydrochloride was used as the chromogen. All sections were counterstained with haematoxylin for 1 minute.

Morphometric methods

Protein deposits in AD and vCJD have a similar morphology [2,9]. In both disorders, there are diffuse deposits (also known in vCJD as 'fine feathery diffuse deposits' or 'fine diffuse plaques') and more complex deposits in which a distinct central 'core' of Aβ or PrP^{sc} is present and are termed 'classical' plaques in AD or 'florid' plaques in vCJD [9]. Within each gyrus, the greatest diameter of a sample of diffuse and classic/florid deposits was measured. Guidelines were marked on the slide parallel to the pia mater in laminae II/III and V/VI, regions that contain the most significant numbers of deposits [10]. The maximum diameter of each protein deposit touching a guideline was then measured at a magnification of ×400 using an eyepiece micrometer. Diffuse Aβ deposits were 10-200 µm in diameter, irregular in shape with diffuse boundaries and lightly stained, while classic deposits had a distinct central core surrounded by a 'corona' of dystrophic neurites [2]. Florid PrP^{sc} deposits were unicentric and consisted of a dense core, while diffuse deposits were irregularly shaped, more lightly stained than the florid deposits and always lacked a solid core [9]. To obtain a sufficiently large sample of each type of deposit within each disease group to fit a log-normal model, measurements were combined from all brain regions and patients.

Data analysis

A log-normal model was fitted to the size distribution of each type of deposit [35] using STATISTICA software (Statsoft Inc., 2300 East 14th St, Tulsa, OK 74104, USA). The log-normal distribution is defined as that of a variable X such that ln (X-Ø) is normally distributed. The distribution has three parameters: Ø (where X > Ø), the mean (μ), and the variance (σ2). In many applications, the value of Ø can be assumed to be zero and a two-parameter model fitted to the data. Deviations from a log-normal model were tested using the Kolmogorov-Smirnov (KS) goodness-of-fit test.

Results

The size frequency distributions of the Aβ deposits are shown in Figures 1 and 2 and the PrP^{sc} deposits in Figures 3 and 4. The mean size, modal class, standard deviation, maximum size and degree of skew of the distributions are summarised in Table II. All size distributions were unimodal and positively skewed. There were few deposits represented in the smallest size classes, maximum frequency occurred at upper

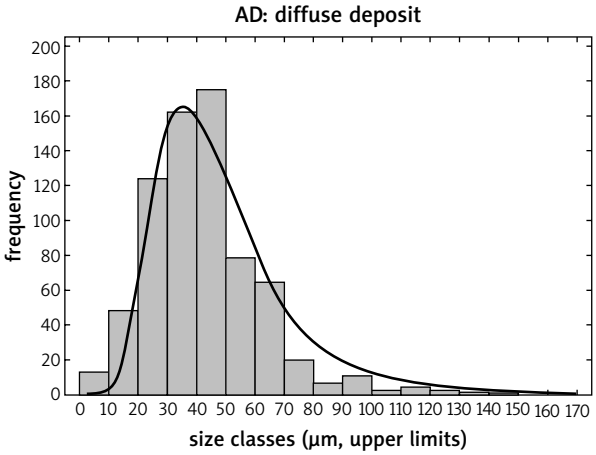

Fig. 1. Size frequency distribution of diffuse-type β-amyloid (Aβ) deposits in the temporal lobe in sporadic Alzheimer's disease (Kolmogorov-Smirnov (KS) test of goodness-of-fit to a log-normal distribution = 0.10, P<0.01)

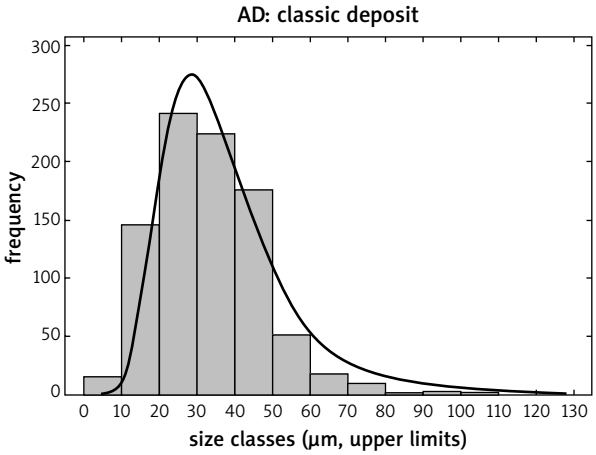

Fig. 2. Size frequency distribution of the classic-type β-amyloid (Aβ) deposits in the temporal lobe in sporadic Alzheimer's disease (KS=0.09, P<0.01)

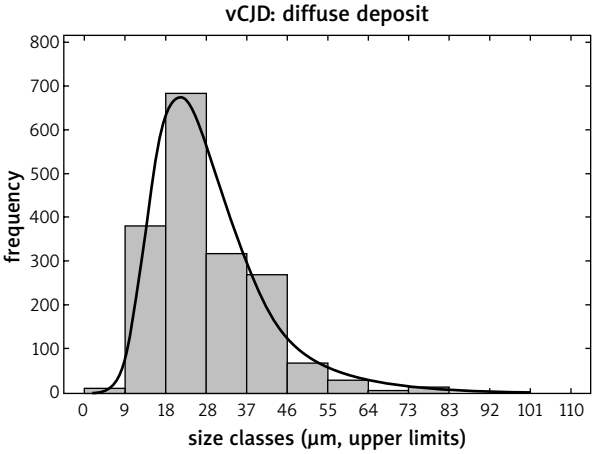

Fig. 3. Size frequency distribution of the diffuse-type prion protein (PrP^{sc}) deposits in the temporal lobe in variant Creutzfeldt-Jakob disease (vCJD) (KS=0.03, P>0.05)

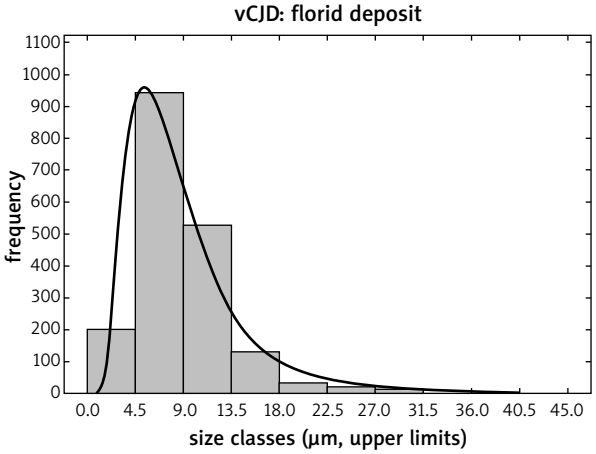

Fig. 4. Size frequency distribution of the florid-type prion protein (PrP^{sc}) deposits in the temporal lobe in variant Creutzfeldt-Jakob disease (vCJD) (KS=0.10, P<0.01)

Table II. Summary statistics for the size frequency distributions of the Aβ and prion protein deposits in cases of sporadic Alzheimer's disease (AD) and variant Creutzfeldt-Jakob disease (vCJD) respectively (** – P<0.01)

Distribution statistics							
Group	**Deposit Type**	**N**	**Mean (µm)**	**Mode (µm)**	**SD (µm)**	**Max (µm)**	**Degree of Skew**
AD	Diffuse	715	47.22	50	20.01	150	1.20**
	Classic	888	37.02	30	14.52	110	0.88**
vCJD	Diffuse	1782	27.85	25	12.03	100	1.53**
	Florid	1887	8.56	5	4.98	37.50	1.62**

N – number of deposits sampled; SD – standard deviation; Max – maximum size of deposit.

boundary sizes of 30-50 µm (the modal class) for the Aβ deposits and 5-25 µm for the PrP^{sc} deposits, while the frequency of the larger deposits declined rapidly with increasing size. Average and maximum diameter of the diffuse Aβ deposits was greater than that of the corresponding diffuse PrP^{sc} deposits, and similarly, the classic Aβ deposits were larger than the florid PrP^{sc} deposits. The PrP^{sc} deposits had smaller standard deviations but exhibited a greater degree of skew than the Aβ deposits.

All distributions were approximately log-normal in shape. However, with the exception of the diffuse deposits in vCJD (Fig. 3), the distributions showed some deviations from the expected numbers of deposits predicted by the log-normal model. Hence, there were more diffuse Aβ deposits (Fig. 1) with an upper size limit of <50 µm in diameter and fewer >50 µm than expected and there were more classic Aβ deposits (Fig. 2) <20 µm and fewer between 20 µm and 40 µm than expected, while the numbers of deposits >60 mm were closer to those predicted by the log-normal model. There were fewer florid PrP^{sc} deposits (Fig. 4) <4.5 µm, more in the modal class (5 µm), and fewer >18 µm than predicted by the log-normal model.

Discussion

Both Aβ and PrP^{sc} deposits exhibited a unimodal, positively skewed size distribution, suggesting similarities in the growth phase of both types of deposit. The average and maximum size of the Aβ deposits, however, was significantly greater than the analogous PrP^{sc} deposits. Either Aβ deposits increase in size

more rapidly or develop over a much longer time period than PrP^{sc} deposits. Although vCJD cases have a duration of up to two years, considerably longer than in sporadic CJD [43], duration of disease is still much shorter than in AD. However, in the AD cases with a short duration (2-3 yrs), the sizes of the Aβ deposits were still significantly greater than those of the PrP^{sc} deposits, suggesting that Aβ deposits have an intrinsically greater growth potential. In addition, the PrP^{sc} deposits exhibit a greater degree of skew and smaller standard deviations than the Aβ deposits. This suggests that the pattern of growth of the PrP^{sc} deposits is less variable than the Aβ deposits and that there are factors that restrict the growth of the PrP^{sc} deposits to within a certain size range.

Development of protein deposits is characterised by two processes, viz., growth and removal of protein molecules (aggregation/disaggregation) and the diffusion of substances into the deposit (surface diffusion) [38,41]. The size frequency distribution approaches log-normal if surface diffusion predominates over that of aggregation/disaggregation. In a previous study [12], the distributions of the diffuse and the florid PrP^{sc} deposits deviated significantly from a log-normal model. The present data, comprising a large sample of deposits from the temporal lobe, differ in that the diffuse PrP^{sc} deposits did not deviate significantly from a log-normal distribution. Hence, surface diffusion may be important in the development of the diffuse deposits. Diffuse deposits may acquire small molecular weight ligand substances readily, the substances contributing to growth by binding to PrP^{sc} and promoting the formation of peptide bonds [28]. For example, clusterin is a heterodimeric glycoprotein which has a propensity to form aggregates and which can interact with PrP^{sc} [17]. Compliment activation products C1q and C3d, serum amyloid P, and activated glial cells may also accumulate in prion deposits and influence their growth and development [42]. These substances are also found in diffuse Aβ deposits [4] but may have little effect on the growth phase.

The remaining size distributions deviated from a log-normal model. Most notably, there were far fewer florid PrP^{sc} deposits in the smallest size class (<4.5 μm) than predicted. Sampling in two dimensions underestimates the frequency of small deposits [6,25] and this sampling error may be particularly significant in measuring the small florid deposits. Alternatively, fibril formation is nucleation dependent and occurs after a lag time which decreases with increasing peptide concentration [33]. Once small amorphous aggregates are formed and β-sheet formation is initiated there is rapid growth of the stable fibrils or protofibrils to form the deposits [33]. Hence, rapid early growth of the florid deposits could also explain the low numbers of small deposits observed.

There were fewer of the large diffuse Aβ and florid PrP^{sc} deposits than predicted by the log-normal model, consistent with the suggestion that there is an upper limit to the growth of these deposits. During the growth phase of Aβ deposits, new amyloid fibres are formed at the periphery of existing deposits [44] with specific amyloid aggregate formation accelerated by the homogeneous association of soluble $A\beta_{42}$ onto existing $A\beta_{42}$ seeds [18]. By contrast, growth of a PrP^{sc} deposit is dependent on the continued autocatalytic conversion of PrP^{c}. Hence, growth of a deposit will depend on a supply of the precursors of Aβ and PrP^{sc}, viz., amyloid precursor protein (APP) and PrP^{c} respectively, both of which are neuronal proteins of uncertain function. The size of an Aβ deposit is positively correlated with the number of associated neuronal perikarya [6]. Hence, deposit size may be restricted by the number of immediately adjacent neurons that degenerate and secrete the proteins necessary to form the deposit (Armstrong et al., 1997). Furthermore, both the classic deposits in AD [1,5] and the florid deposits in vCJD [11] have been observed to cluster around the vertically penetrating arterioles in the upper laminae of the cerebral cortex, suggesting that factors associated with blood vessels or blood are important. Substances diffusing from blood into the brain as a result of an impaired blood brain barrier might encourage condensation of the protein to form a dense core, thus restricting the size of the deposit [11].

The role of aggregated proteins in the pathogenesis of AD and CJD is controversial. The aggregates themselves may be toxic and therefore these results may be useful in the design of treatments that may act to restrict their growth and spread. Alternatively, in AD, Aβ oligomer intermediates may be the toxic species [26] and amyloid formation and deposit growth could represent a protective mechanism that actually removes the toxic species from the brain [15]. In this case, studies of the size frequency distributions of protein deposits may be a useful means of studying this potentially important protective mechanism.

Acknowledgements

The assistance of the Brain Bank, Institute of Psychiatry, King's College London in preparation of tissue sections for this study is gratefully acknowledged. The CJD Surveillance Unit is supported by the Department of Health, the Scottish Executive and TSELAB Project of the EC (reference QLK2-CT-2002--81523).

References

1. Armstrong RA. Is the clustering of β-amyloid (Aβ) deposits in the frontal cortex of Alzheimer patients determined by blood vessels? Neurosci Lett 1995; 195: 121-124.
2. Armstrong RA. β-amyloid plaques: stages in life history or independent origin? Dement Geriatr Cogn Disord 1998; 9: 227-238.
3. Armstrong RA. Do β-amyloid (Aβ) deposits in patients with Alzheimer's disease and Down's syndrome grow according to the log-normal model? Neurosci Lett 1999; 261: 97-100.
4. Armstrong RA. Plaques and tangles and the pathogenesis of Alzheimer's disease. Folia Neuropathol 2006; 44: 1-11.
5. Armstrong RA. Classic β-amyloid deposits cluster around large diameter blood vessels rather than capillaries in sporadic Alzheimer's disease. Curr Neurovasc Res 2006; 3: 289-294.
6. Armstrong RA, Myers D, Smith CU. Factors determining the size frequency distribution of β-amyloid (Aβ) deposits in Alzheimer's disease. Exp Neurol 1997; 145: 574-579.
7. Armstrong RA, Lantos PL, Cairns NJ. The spatial patterns of prion protein deposits in Creutzfeldt-Jakob disease: comparison with β-amyloid deposits in Alzheimer's disease. Neurosci Lett 2001; 298: 53-56.
8. Armstrong RA, Cairns NJ, Ironside JW, Lantos PL. Quantification of vacuolation ("spongiform change"), surviving neurones and prion protein deposition in eleven cases of variant Creutzfeldt--Jakob disease. Neuropathol Appl Neurobiol 2002; 28: 129-135.
9. Armstrong RA, Cairns NJ, Ironside JW, Lantos PL. Laminar distribution of the pathological changes in the cerebral cortex in variant Creutzfeldt-Jakob disease (vCJD). Folia Neuropathol 2002; 40: 165-171.
10. Armstrong RA, Lantos PL, Ironside JW, Cairns NJ. Differences in the density and spatial distribution of florid and diffuse plaques in variant Creutzfeldt-Jakob disease (vCJD). Clin Neuropathol 2003; 22: 209-214.
11. Armstrong RA, Cairns NJ, Ironside JW, Lantos PL. Florid prion protein (PrP) plaques in patients with variant Creutzfeldt-Jakob disease (vCJD) are spatially related to blood vessels. Neurosci Res Communs 2003; 32: 29-36.
12. Armstrong RA, Cairns NJ, Ironside JW, Lantos PL. Size frequency distribution of prion protein (PrP) aggregates in variant Creutzfeldt-Jakob disease. J Neural Transm 2005; 112: 1565-1573.
13. Benes FM, Reifel JL, Majocha RE, Marotta CA. Evidence for a diffusional model of Alzheimer amyloid A4 (β amyloid) during neuritic plaque formation. Neuroscience 1989; 33: 483-488.
14. Braak H, Braak E. Neuropathological stageing of Alzheimer-related changes. Acta Neuropathol (Berl) 1991; 82: 239-259.
15. Carrotta R, Manno M, Bulone D, Martorana V, San Biagio PL. Protofibril formation of amyloid beta-protein at low pH via a non-cooperative elongation mechanism. J Biol Chem 2005; 280: 30001-30008.
16. Christopeit T, Hortschansky P, Schroeckh V, Guhrs K, Zandomeneghi G, Fandrich M. Mutagenic analysis of the nucleation propensity of oxidized Alzheimer's beta-amyloid peptide. Protein Sci 2005; 14: 2125-2131.
17. Freixes M, Puig B, Rodríguez A, Torrejón-Escribano B, Blanco R, Ferrer I. Clusterin solubility and aggregation in Creutzfeldt-Jakob disease. Acta Neuropathol (Berl) 2004; 108: 295-301.
18. Ha C, Park CB. Ex situ atomic force microscopy analysis of beta--amyloid self-assembly and deposition on a synthetic template. Langmuir 2006; 22: 6977-6985.
19. El Hachini KH, Cervenakova L, Brown P, Goldfarb LG, Rubenstein R, Gajdusek DC, Foncin JF. Mixed features of Alzheimer's disease and Creutzfeldt-Jakob disease in a family with a presenilin 1 mutation in chromosome 14. Amyloid: Int J Exp Clin Invest 1996; 3: 223-233.
20. Hainfellner JA, Wanschitz J, Jellinger K, Liberski PP, Gullota F, Budka H. Coexistence of Alzheimer-type neuropathology in Creutzfeldt-Jakob disease. Acta Neuropathol (Berl) 1998; 96: 116-122.
21. Harper JD, Lansbury PT Jr. Models of amyloid seeding in Alzheimer's disease and scrapie: mechanistic truths and physiological consequences of the time-dependent solubility of amyloid proteins. Annu Rev Biochem 1997; 66: 385-407.
22. Hill AF, Butterworth RJ, Joiner S, Jackson G, Rossor MN, Thomas DJ, Frosh A, Tolley N, Bell JE, Spencer M, King A, Al-Sarraj S, Ironside JW, Lantos PL, Collinge J. Investigation of variant Creutzfeldt-Jakob disease and other human prion diseases with tonsil biopsy samples. Lancet 1999; 353: 183-189.
23. Hyman BT, West HL, Rebeck GW, Buldyrev SV, Mantegna RN, Ukleja M, Havlin S, Stanley HE. Quantitative analysis of senile plaques in Alzheimer disease: observation of log-normal size distribution and molecular epidemiology of differences associated with apolipoprotein E genotype and trisomy 21 (Down syndrome). Proc Natl Acad Sci U S A 1995; 92: 3586-3590.
24. Ironside JW, Head MW, Bell JE, McCardle L, Will RG. Laboratory diagnosis of variant Creutzfeldt-Jakob disease. Histopathology 2000; 37: 1-9.
25. Kawai M, Cras P, Perry G. Serial reconstruction of β-protein amyloid plaques: relationship to microvessels and size distribution. Brain Res 1992; 592: 278-282.
26. Kim JR, Muresan A, Lee KY, Murphy RM. Urea modulation of beta-amyloid fibril growth: experimental studies and kinetic models. Protein Sci 2004; 13: 2888-2898.
27. Krasemann S, Groschup MH, Harmeyer S, Hunsmann G, Bodemer W. Generation of monoclonal antibodies against human prion proteins in PrP0/0 mice. Mol Med 1996; 2: 725-734.
28. Kuner P, Bohrmann B, Tjernberg LO, Näslund J, Huber G, Celenk S, Gruninger-Leitch F, Richards JG, Jakob-Roetne R, Kemp JA, Nordstedt C. Controlling polymerization of beta-amyloid and prion-derived peptides with synthetic small molecule ligands. J Biol Chem 2000; 275: 1673-1678.
29. Li G, Zhou P, Shao Z, Xie X, Chen X, Wang H, Chunyu L, Yu T. The natural silk spinning process. A nucleation-dependent aggregation mechanism? Eur J Biochem 2001; 268: 6600-6606.

30. Maggio JE, Stimson ER, Ghilardi JR, Allen CJ, Dahl CE, Whitcomb DC, Vigna SR, Vinters HV, Labenski ME, Mantyh PW. Reversible in vitro growth of Alzheimer disease beta-amyloid plaques by deposition of labeled amyloid peptide. Proc Natl Acad Sci U S A 1992; 89: 5462-5466.
31. Mirra SS, Heyman A, McKeel D, Sumi SM, Crain BJ, Brownlee LM, Vogel FS, Hughes JP, van Belle G, Berg L. The Consortium to Establish a Registry for Alzheimer's Disease (CERAD). Part II. Standardization of the neuropathologic assessment of Alzheimer's disease. Neurology 1991; 41: 479-486.
32. Muramoto T, Kitamoto T, Koga H, Tateishi J. The coexistence of Alzheimer's disease and Creutzfeldt-Jakob disease in a patient with dementia with long duration. Acta Neuropathol (Berl) 1992; 84: 686-689.
33. Nguyen HD, Hall CK. Kinetics of fibril formation by polyalanine peptides. J Biol Chem 2005; 280: 9074-9082.
34. Preusser M, Strobel T, Gelpi E, Eiler M, Broessner G, Schmutzhard E, Budka H. Alzheimer-type neuropathology in a 28 year old patient with iatrogenic Creutzfeldt-Jakob disease after dural grafting. J Neurol Neurosurg Psychiatry 2006; 77: 413-416.
35. Pollard JH. Numerical and Statistical Technique. Cambridge University Press, Cambridge 1979.
36. Robbins EM, Betensky RA, Domnitz SB, Purcell SM, Garcia-Alloza M, Greenberg C, Rebeck GW, Hyman BT, Greenberg SM, Frosch MP, Bacskai BJ. Kinetics of cerebral amyloid angiopathy progression in a transgenic mouse model of Alzheimer disease. J Neurosci 2006; 26: 365-371.
37. Spargo E, Luthert PJ, Anderton BH, Bruce M, Smith D, Lantos PL. Antibodies raised against different portions of A4 protein identify a subset of plaques in Down's syndrome. Neurosci Lett 1990; 115: 345-350.
38. Stanley HE, Buldyrev SV, Cruz L, Gomez-Isla T, Havlin S, Hyman BT, Knowles R, Urbanc B, Wyart C. Statistical physics and Alzheimer's disease. Physica A 1998; 249: 460-471.
39. Tierney MC, Fisher RH, Lewis AJ, Zorzitto ML, Snow WG, Reid DW, Nieuwstraten P. The NINCDS-ADRDA work group criteria for the clinical diagnosis of probable Alzheimer's disease. Neurology 1988; 38: 359-364.
40. Urbanc B, Cruz L, Buldyrev SV, Havlin S, Irizarry MC, Stanley HE, Hyman BT. Dynamics of plaque formation in Alzheimer's disease. Biophys J 1999a; 76: 1330-1334.
41. Urbanc B, Cruz L, Buldyrev SV, Havlin S, Hyman BT, Stanley HE. Dynamic feedback in an aggregation-disaggregation model. Physic Rev E 1999b; 60: 2120-2126.
42. Veerhuis R, Boshuizen RS, Morbin M, Mazzoleni G, Hoozemans JJ, Langedijk JP, Tagliavini F, Langeveld JP, Eikelenboom P. Activation of human microglia by fibrillar prion protein-related peptides is enhanced by amyloid-associated factors SAP and C1q. Neurobiol Dis 2005; 19: 273-282.
43. Will RG, Ironside JW, Zeidler M, Cousens SN, Estibeiro K, Alperovitch A, Poser S, Pocchiari M, Hofman A, Smith PG. A new variant of Creutzfeldt-Jakob disease in the UK. Lancet 1996; 347: 921-925.
44. Yamaguchi H, Yamazaki T, Lemere CA, Frosch MP, Selkoe DJ. Beta amyloid is focally deposited within the outer basement membrane in the amyloid angiopathy of Alzheimer's disease. An immunoelectron microscopic study. Am J Pathol 1992; 141: 249-259.